Available online at www.sciencedirect.com

SciVerse ScienceDirect

Procedia IUTAM 7 (2013) 29 – 38

Procedia IUTAM

www.elsevier.com/locate/procedia

Topological Fluid Dynamics: Theory and Applications

Vortex knots dynamics in Euler fluids

Francesca Maggioni[a]*, Sultan Z. Alamri[b], Carlo F. Barenghi[c] and Renzo L. Ricca[d]

[a]*Dept. Mathematics, Statistics, Computer Science and Applications, U. Bergamo, Via dei Caniana 2, 24127 Bergamo, Italy*
[b]*Dept. Applied Mathematics, College of Applied Science, U. Taibah, P.O. Box 344, Al-Madinah Al-Munawarah, Saudi Arabia*
[c] *School of Mathematics and Statistics, U. Newcastle, Newcastle upon Tyne, NE1 7RU, U.K.*
[d]*Department of Mathematics and Applications, University of Milano-Bicocca, Via Cozzi 53, 20125 Milano, Italy*

Abstract

In this paper we examine certain geometric and topological aspects of the dynamics and energetics of vortex torus knots and unknots. The knots are given by small-amplitude torus knot solutions in the local induction approximation (LIA). Vortex evolution is then studied in the context of the Euler equations by direct numerical integration of the Biot-Savart law and the velocity, helicity and kinetic energy of different vortex knots and unknots are presented for comparison. Vortex complexity is parametrized by the winding number w given by the ratio of the number of meridian wraps to longitudinal wraps. We find that for $w < 1$, vortex knots and toroidal coils move faster and carry more energy than a reference vortex ring of the same size and circulation, whereas for $w > 1$, knots and poloidal coils have approximately the same speed and energy as the reference vortex ring. Kinetic helicity is dominated by writhe contributions and increases with knot complexity. All torus knots and unknots tested under Biot-Savart show much stronger permanence than under LIA.

© 2013 The Authors. Published by Elsevier B.V.
Selection and/or peer-review under responsibility of the Isaac Newton Institute for Mathematical Sciences, University of Cambridge

Keywords: vortex knots; helicity; Biot-Savart law; Local Induction Approximation (LIA); topological fluid dynamics.

1. Introduction

The study of in ideal fluids, and in particular of vortex rings in the presence or absence of periodic displacements of the vortex axis from the circular shape (Kelvin waves), dates back to the late 1800s [1]. Despite its long history, this study is still an active area of research [2, 3, 4]. Alongside the traditional interest for problems in classical fluid mechanics, additional interest is motivated by current work on superfluid helium [5, 6, 7, 8] and atomic Bose-Einstein condensates [9, 10, 11].

Here we shall be concerned with knots and unknots in an ideal fluid, identified with closed vortex lines, around which the circulation assumes nonzero (quantized) value. Among all possible knot types, torus knots constitute a special family of knots amenable to particularly simple mathematical description. These knots can be described by closed curves wound on a mathematical torus p times in the longitudinal direction and q times in the meridian

* Corresponding author
E-mail address: francesca.maggioni@unibg.it

2210-9838 © 2013 The Authors. Published by Elsevier B.V.
Selection and/or peer-review under responsibility of the Isaac Newton Institute for Mathematical Sciences, University of Cambridge
doi:10.1016/j.piutam.2013.03.005

direction. If $p > 1$ and $q > 1$ are co-prime integers, then we have torus knots (see Figure 1), otherwise the curve forms an unknot (see Figure 2). Even unknots however, have a rather complex geometry, taking the shape of toroidal and poloidal coils, worth exploring.

In this paper we study numerically the velocity, helicity and stability of vortex knots and unknots by comparing the results with a standard vortex ring of the same size. We adopt the classical theory of a thin-core vortex filament based on the large separation of scales between the vortex core radius a_0 (approximately 10^{-8} cm in ^{4}He) and the typical distance l between vortices; in superfluid turbulence, $l \approx 10^{-3}$ to 10^{-4} cm, where the lower value is also the typical diameter of experimental vortex rings [12]. In this approach, the governing incompressible Euler dynamics is governed by the full Biot-Savart law or, alternatively, by its local induction approximation (see below for its definition). In the LIA context, it has been conjectured [13] and recently proved [14, 15], that any closed curve more complex than a circular ring is linearly unstable to perturbations, changing knot type during evolution. However, in this paper we demonstrate that all knots and unknots tested under Biot-Savart show remarkable persistence in space and time.

Since superfluid ^{4}He has zero viscosity, thus providing a realistic example of an Euler fluid, we shall choose circulation and vortex core radius as physically realistic quantities for quantized vortices in superfluid helium. Moreover, by assuming that no friction force acts on the superfluid vortices [16], our results apply to superfluid helium at temperatures below 1 K, where the dissipative effects of the normal fluid are truly negligible. The situation is very different in atomic Bose-Einstein condensates governed by the Gross-Pitaevskii equation, (GPE) since l is only a few times larger than a_0. In the GPE case there is no need to introduce a cut-off parameter to de-singularize the Biot-Savart integral, and vortex reconnection emerges naturally from that model equation. This means that while GPE conserves total kinetic energy (as in the Euler and superfluid case), topology is allowed to change. The existence and evolution of vortex knots in the GPE model has been studied by [17], by focusing on the two simplest vortex knots $\mathcal{T}_{2,3}$ and $\mathcal{T}_{3,2}$. It has been found that for small knot ratios both $\mathcal{T}_{2,3}$ and $\mathcal{T}_{3,2}$ behave similarly and are long-lived structures, preserving their shape in time.

2. Mathematical background

2.1. Vortex motion under Biot-Savart and LIA law

We consider vortex motion in an ideal, incompressible fluid, in an unbounded domain. The velocity field $\mathbf{u} = \mathbf{u}(\mathbf{x}, t)$, a smooth function of the vector position $\mathbf{x}$ and time t, satisfies

$$\nabla \cdot \mathbf{u} = 0 \quad \text{in } \mathbb{R}^3 , \qquad \mathbf{u} \to 0 \quad \text{as } \mathbf{x} \to \infty , \tag{1}$$

with vorticity $\boldsymbol{\omega}$ defined by

$$\boldsymbol{\omega} = \nabla \times \mathbf{u} , \qquad \nabla \cdot \boldsymbol{\omega} = 0 \quad \text{in } \mathbb{R}^3 . \tag{2}$$

In the absence of dissipation, physical properties such as kinetic energy, helicity and momenta are therefore conserved along with topological quantities such as knot type, minimum crossing number and self-linking number. The kinetic energy per unit density E is given by

$$E = \frac{1}{2} \int_V |\mathbf{u}|^2 \, \mathrm{d}^3\mathbf{x} = \text{constant} , \tag{3}$$

where V is the fluid volume, and the kinetic helicity H by

$$H = \int_V \mathbf{u} \cdot \boldsymbol{\omega} \, \mathrm{d}^3\mathbf{x} = \text{constant} . \tag{4}$$

Here we assume to have only one vortex filament $\mathcal{F}$ in isolation, where $\mathcal{F}$ is centered on the curve $\mathcal{C}$ of equation $\mathbf{X} = \mathbf{X}(s)$ (s being the arc-length of $\mathcal{C}$). The filament axis $\mathcal{C}$ is given by a smooth (that is at least C^2), simple (i.e. without self-intersections), space curve $\mathcal{C}$. The filament volume is given by $V(\mathcal{F}) = \pi a^2 L$, where $L = L(\mathcal{C})$ is the total length of $\mathcal{C}$ and a is the radius of the vortex core, assumed to be uniformly circular all along $\mathcal{C}$ and much smaller than any length scale of interest in the flow (thin-filament approximation); this assumption is relevant (and particularly realistic) in the context of superfluid helium vortex dynamics, where typically $a \approx 10^{-8}\mathrm{cm}$.

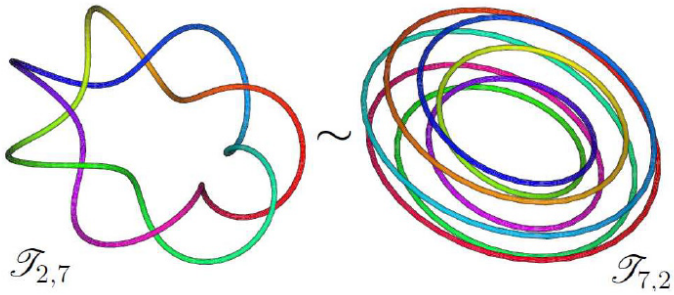

Fig. 1. Examples of torus knots with winding number $w > 1$ (left) and $w < 1$ (right). The knots $\mathcal{T}_{2,7} \sim \mathcal{T}_{7,2}$ are topologically equivalent.

Vortex motion is governed by the Biot-Savart law (BS for short) given by

$$\mathbf{u}(\mathbf{x}) = \frac{\Gamma}{4\pi} \oint_{\mathcal{C}} \frac{\hat{\mathbf{t}} \times (\mathbf{x} - \mathbf{X}(s))}{|\mathbf{x} - \mathbf{X}(s)|^3} \, \mathrm{ds} \,, \tag{5}$$

where Γ is the vortex circulation due to $\boldsymbol{\omega} = \omega_0 \hat{\mathbf{t}}$, where ω_0 is a constant and $\hat{\mathbf{t}} = \hat{\mathbf{t}}(s) = \mathrm{d}\mathbf{X}/\mathrm{ds}$ the unit tangent to $\mathcal{C}$. Since the Biot-Savart integral is a global functional of vorticity and geometry, analytical solutions in closed form other than the classical solutions associated with rectilinear, circular and helical geometry are very difficult to obtain. Considerable analytical progress, however, has been made by using the Localized Induction Approximation (LIA) law [18]. By neglecting the rotational component of the self-induced velocity (that in any case does not contribute to the displacement of the vortex filament in the fluid) and non-local terms, the LIA equation takes the simplified form

$$\mathbf{u}_{\mathrm{LIA}} = \frac{\Gamma c}{4\pi} \ln \delta \, \hat{\mathbf{b}} \propto c \, \hat{\mathbf{b}} \,, \tag{6}$$

where $c = c(s)$ is the local curvature of $\mathcal{C}$, δ is a measure of the aspect ratio of the vortex, given by the radius of curvature divided by the vortex core radius and $\hat{\mathbf{b}} = \hat{\mathbf{b}}(s)$ the unit binormal vector to $\mathcal{C}$.

2.2. LIA torus knots

We consider torus knots in $\mathbb{R}^3$. These are given by a curve $\mathcal{C}$ in the shape of a torus knot $\mathcal{T}_{p,q}$ ((p, q) co-prime integers, with $p > 1$ and $q > 1$), drawn on a mathematical torus p times in the longitudinal (toroidal) direction and q times in the meridian (poloidal) direction (see Figure 1). When one of the integers equals 1 and the other m, then the curve is no longer knotted, but it forms an unknot homeomorphic to the standard circle $\mathcal{U}_0$. Depending on the index, the curve may take the shape of a toroidal coil $\mathcal{U}_{m,1}$, or a poloidal coil $\mathcal{U}_{1,m}$ (see Figure 2). When p and q are both rational, then $\mathcal{T}_{p,q}$ is no longer a closed knot, the curve covering the toroidal surface completely. Here we shall consider only curves given by (p, q) integers. The *winding number* is given by the ratio $w = q/p$ and the *self-linking number* is given by $Lk = pq$, two topological invariants of $\mathcal{T}_{p,q}$. Note that for given p and q the knot $\mathcal{T}_{p,q}$ is topologically equivalent to $\mathcal{T}_{q,p}$, that is $\mathcal{T}_{p,q} \sim \mathcal{T}_{q,p}$, i.e. both represent the same knot type, even though their geometry is completely different.

A useful measure of geometric complexity of $\mathcal{C}$ is given by the *writhing number* [19] defined by

$$Wr\,(\mathcal{C}) \equiv \frac{1}{4\pi} \oint_{\mathcal{C}} \oint_{\mathcal{C}} \frac{\hat{\mathbf{t}}(s) \times \hat{\mathbf{t}}(s^*) \cdot [\mathbf{X}(s) - \mathbf{X}(s^*)]}{|\mathbf{X}(s) - \mathbf{X}(s^*)|^3} \, \mathrm{ds} \, \mathrm{ds}^* \,, \tag{7}$$

where $\mathbf{X}(s)$ and $\mathbf{X}(s^*)$ denote two points on the curve $\mathcal{C}$ for any pair $\{s, s^*\} \in [0, L]$, the integration being performed twice on the same curve $\mathcal{C}$. The writhing number provides a direct measure of coiling and distortion of the filament in space. This information can be related to the *total twist number* Tw and, by knowing the self-linking number Lk of each knot, to the helicity H of the vortex, given by [20]Ricca, R.L.Moffatt, H.K.

$$H = \Gamma Lk = \Gamma(Wr + Tw) \,, \tag{8}$$

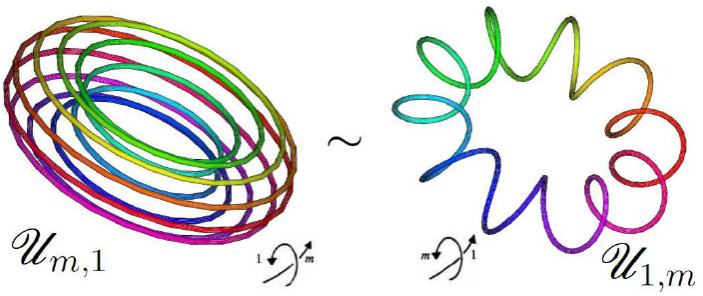

Fig. 2. Examples of torus unknots with winding number $w > 1$ (poloidal coils; left) and $w < 1$ (toroidal coils; right). These unknots with $m > 1$ are both homeomorphic to the standard circle.

where we used the Călugăreanu-White formula $Lk = Wr + Tw$.

Hereafter we shall refer to $\mathcal{T}_{p,q}$ as the vortex torus knot, and study dynamical and energetic properties by using the BS law (5) and the LIA law (6). The existence of torus knot solutions to LIA were found by KidaKida, S. [21] in terms of elliptic integrals. By re-writing LIA in cylindrical polar coordinates (r, α, z), and by using standard linear perturbation techniques, small-amplitude torus knot solutions (asymptotically equivalent to Kida's solutions) were derived by Ricca [22]. These latter give solution curves explicitly in terms of the arc-length s, given by

$$\begin{cases} r = r_0 + \epsilon \sin(w\phi) \, , \\ \alpha = \dfrac{s}{r_0} + \dfrac{\epsilon}{w r_0} \cos(w\phi) \, , \\ z = \dfrac{t}{r_0} + \epsilon \left(1 + \dfrac{1}{w^2}\right)^{1/2} \cos(w\phi) \, , \end{cases} \tag{9}$$

where r_0 is the radius of the torus circular axis and $\epsilon \ll 1$ is the inverse of the aspect ratio of the vortex. Since LIA is related to the one-dimensional Non-Linear Schrödinger Equation (NLSE), torus knot solutions (9) correspond to small amplitude helical travelling waves propagating along the filament axis, with wave speed κ and phase $\phi = (s - \kappa t)/r_0$. Vortex motion is given by a rigid body translation and rotation, with translation velocity $u = \dot{z}$ along the torus central axis and a uniform helical motion along the circular axis of the torus given by radial and angular velocity components $\dot{r}$ and $\dot{\alpha}$. In physical terms, these waves provide an efficient mechanism for the transport of kinetic energy and momenta throughout the fluid.

By using eqs. (9), Ricca [23] proved the following linear stability result:

Theorem (Ricca, 1995): *Let $\mathcal{T}_{p,q}$ be a small-amplitude vortex torus knot under LIA. Then $\mathcal{T}_{p,q}$ is steady and stable under linear perturbations if and only if $q > p$ ($w > 1$).*

This result provides a criterion for LIA stability of vortex knots, and it can be easily extended to inspect stability of torus unknots (i.e. toroidal and poloidal coils). This stability result has been confirmed for the knot types tested by numerical experiments [24]Barenghi, C.F.Samuels, D,C.. Interestingly, though, torus knots that are LIA-unstable are found to have under Biot-Savart a much longer life-time, due evidently to the non-local induction effects. This unexpected result has motivated further work.

3. Numerical method

Dynamical quantities of vortex knots and unknots are evaluated by direct numerical integration of the BS law (5). Numerical work has been carried out by setting $r_0 = 1$ cm (our code works with CGS units), $\epsilon = 0.1$, $\Gamma = 10^{-3}$ cm^2/s, (the value expected for superfluid ^{4}He), $\delta \gg 1$ (in our code $\delta = 2 \cdot 10^8/e^{1/2}$) and, to study unknots, by replacing $(1 - 1/w^2)$ with $|1 - 1/w^2|$ in eqs. (9). It is useful to compare these results with the dynamics of a vortex ring of the same size and vorticity. Thus a reference vortex ring $\mathcal{U}_0$ is taken with radius $r_0 = 1$ cm. The vortex

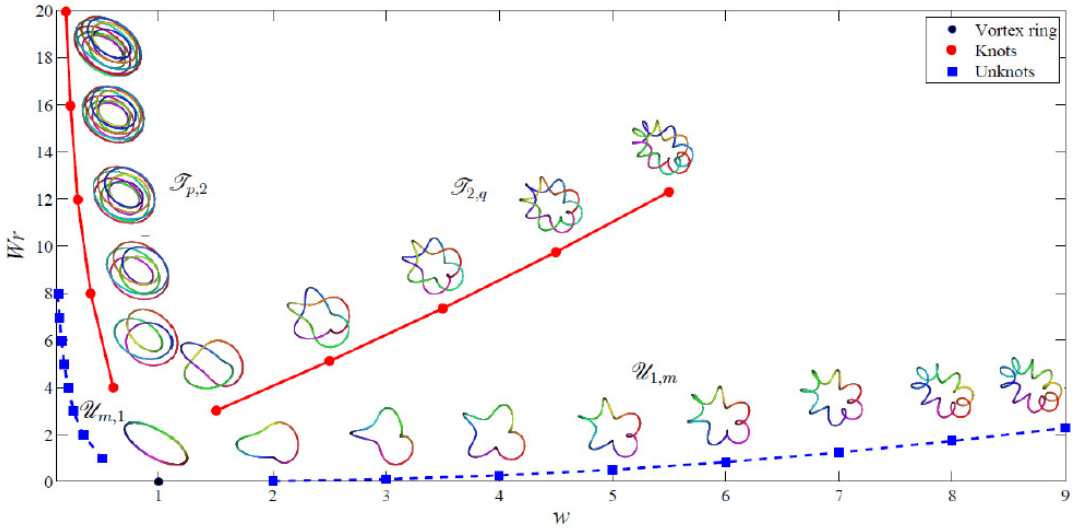

Fig. 3. Comparative analysis of the writhing number Wr plotted against the winding number w of the torus knots and unknots considered ($p = 3, 5, 7, 9$; $q = 3, 5, 7, 9$; $m = 2, 3, \ldots, 7$). Interpolation lines are for visualization purposes only.

axis is discretized into N segments and the Biot-Savart integral is de-singularized by application of a standard cut-off technique [25]. The time evolution is realized by using a 4^{th} order Runge-Kutta algorithm. Convergence has been tested in space and time by modifying discretization points and time steps.

The typical time-step in our calculations is 10^{-2} s. Convergence in time has been tested by varying the time-step from 10^{-3} s to 5×10^{-2} s and using constant mesh density N/L ranging from 7 to 50 according to the different type of toroidal/poloidal knots or unknots. Further details on the constants of calculations are described in [26, 27]Maggioni, F.Alamri, S.Z..

4. Results: helicity, velocity and energy

4.1. Writhing number, total twist number and helicity

First we consider geometric properties such as writhing number and total twist number (see Figures 3−4). As we can see from the diagrams of Figure 3, the dominant contribution to the writhe of the filament comes from the longitudinal wraps, whereas meridian wraps contribute modestly. A useful measure of the total torsion and internal twist of the vortex filament in space is given by the total twist number (see Figure 4), that can be easily computed from the the Călugăreanu-White formula by taking $Tw = Lk - Wr$. Furthermore, by using (8) we have an immediate estimate of the relative contributions to helicity [20]: from the helicity decomposition in writhe and twist contributions, we see that for poloidal representations of knots, that is for $\mathcal{T}_{p,q}$ with $q > p$, writhe and twist helicity increase proportionately with the relative number of wraps, whereas for toroidal representations of knots, such as those given by the $\mathcal{T}_{p,2}$ ($p > 2$), twist helicity remains almost constant, and any increase in linking number is mostly reflected in an increase in writhe helicity. For the unknots it is convenient to set $Lk = 0$, hence $Tw = -Wr$, to estimate writhe and twist helicity contributions.

4.2. Translation velocity

The diagrams of Figure 5 show the velocity u along the central axis of knots and unknots calculated by using the Biot-Savart law against the winding number. The velocity is greatly influenced by the relative number of longitudinal wraps, that contribute dominantly to the total curvature of the vortex. In general the velocity decreases with increasing winding number. Fastest systems are thus the torus knots with the highest number of longitudinal wraps. In the case

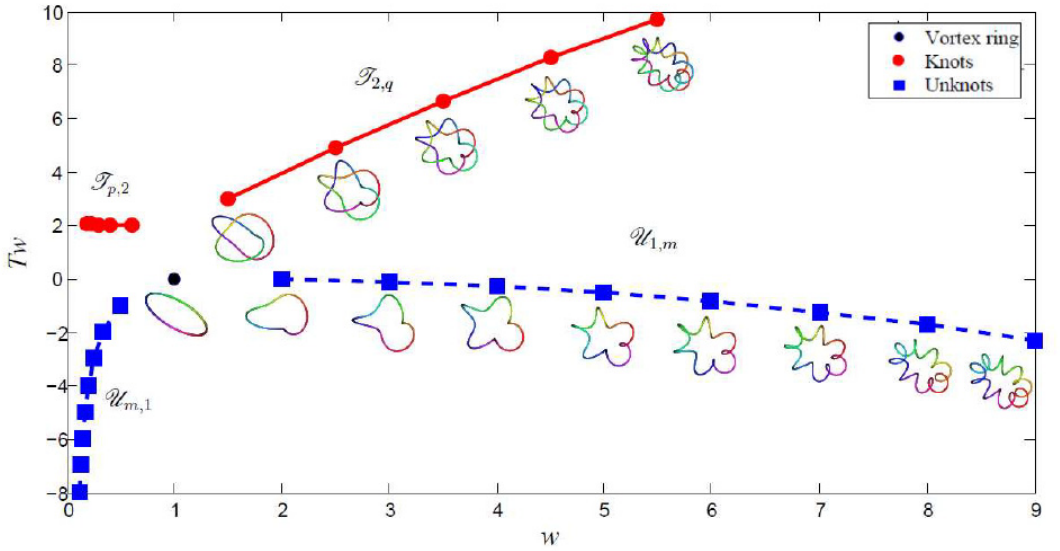

Fig. 4. Comparative analysis of the total twist number Tw plotted against the winding number w of the torus knots and unknots considered ($p = 3, 5, 7, 9$; $q = 3, 5, 7, 9$; $m = 2, 3, \ldots, 7$). Interpolation lines are for visualization purposes only.

of unknots we can see that meridian wraps actually slow down poloidal coils $\mathcal{U}_{1,m}$, by making them traveling slower than the corresponding vortex ring. At very high winding number, torus knots and poloidal coils tend to reverse their velocity, thus traveling backward in space.

The influence of topology on the velocity is investigated in Figure 6, by comparing the velocity of a torus knot and that of the corresponding unknot with same number of longitudinal or meridian wraps. In general vortex knots travel faster than their corresponding unknots, with faster motion for higher number of longitudinal wraps, whereas higher number of meridian wraps slow down the speed.

4.3. Kinetic energy

Let E_0 be the energy of the reference vortex ring. The diagrams of the normalized kinetic energy per unit density E/E_0 of the knots and unknots calculated by using the Biot-Savart law and by the LIA law (E_{LIA}/E_0) are plotted in Figures 7 against the winding number w. The numerical computation of the volume integral (3) is replaced by the line integral [28]

$$E = \frac{\Gamma}{2} \oint_{\mathcal{C}} \mathbf{u} \cdot \mathbf{X} \times \hat{\mathbf{t}} \, \mathrm{d}s \,, \tag{10}$$

where the vorticity contribution is given by the vortex circulation Γ.

Different trends and values are obtained by calculating the normalized energy by using the LIA law; in this case, by using (6), we have

$$E_{\mathrm{LIA}} = \frac{1}{2} \int_V |\mathbf{u}_{\mathrm{LIA}}|^2 \, \mathrm{d}^3\mathbf{x} = \left(\frac{\Gamma \ln \delta}{4\pi} \right)^2 \oint_{\mathcal{C}} \mathrm{c}^2 \, \mathrm{d}s \,, \tag{11}$$

that is one of the conserved quantities associated with the LIA law [22]. Direct comparison between the diagrams of the two energies reveals two distinct trends: for $w < 1$ the LIA law under-estimates the actual energy of the vortex (knotted or unknotted), whereas for $w > 1$ the LIA provides much higher energy values. The influence of non-local effects is evident: the LIA energy of $\mathcal{T}_{9,2}$ and $\mathcal{U}_{7,1}$, for example, is about 40% less than the corresponding BS energy, whereas $\mathcal{T}_{2,9}$ and $\mathcal{U}_{1,7}$ under LIA have 3 and 14 times more energy than their corresponding BS counterparts. These

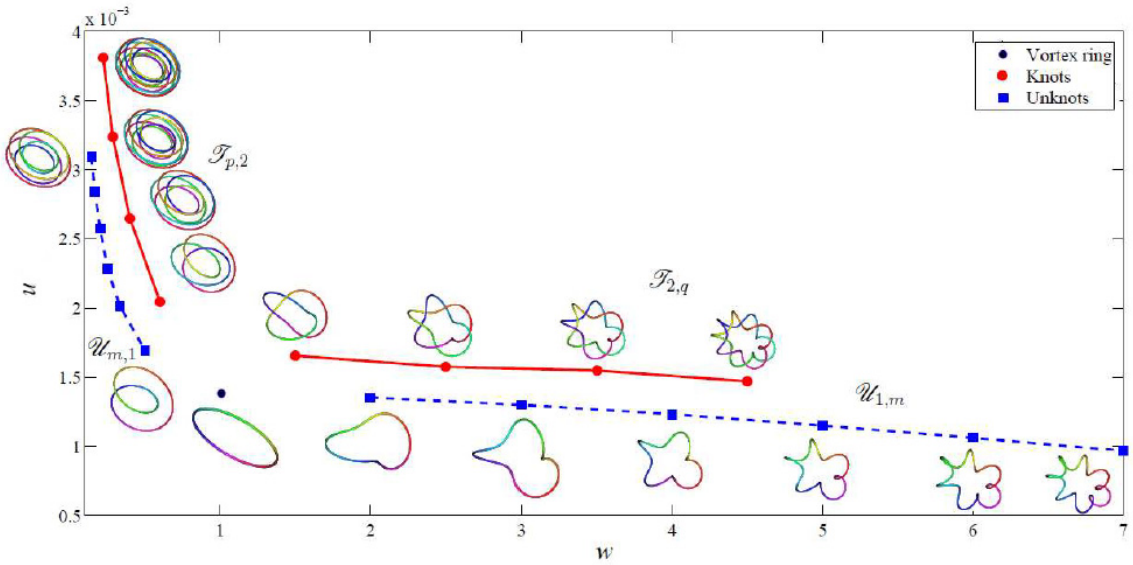

Fig. 5. Torus knots and unknots translational velocity u plotted against the winding number w ($p = 3, 5, 7, 9$; $q = 3, 5, 7, 9$; $m = 2, 3, \ldots, 7$). Interpolation lines are for visualization purposes only.

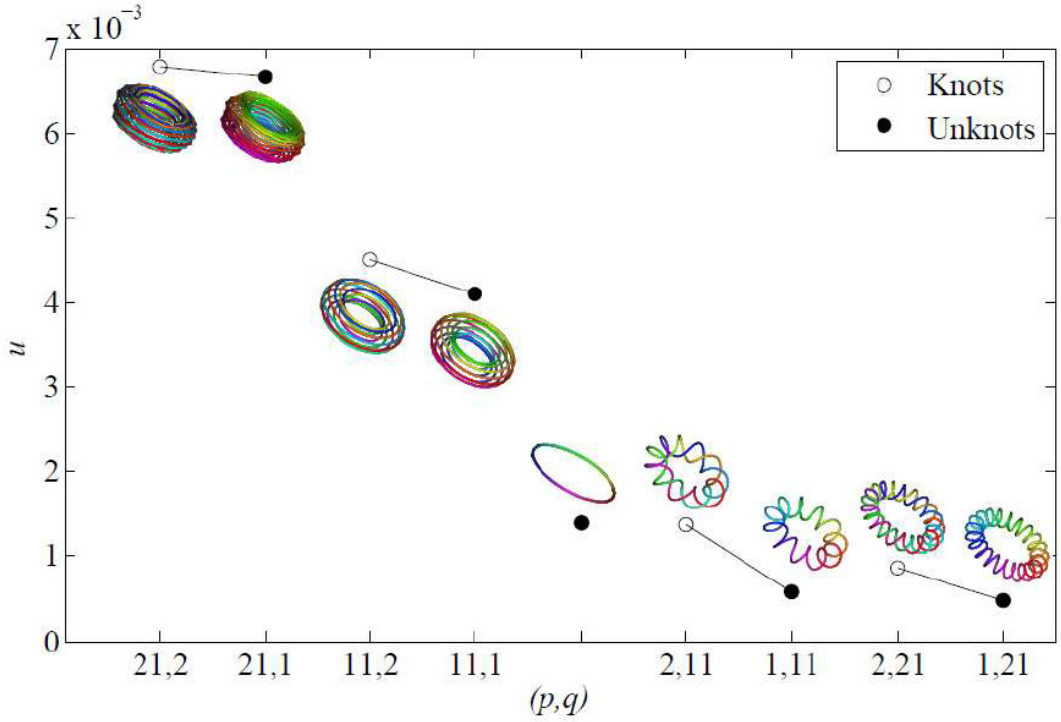

Fig. 6. Translational velocity u of some knots and related unknots. In general knot types travel faster than their corresponding unknots. Interpolation lines are for visualization purposes only.

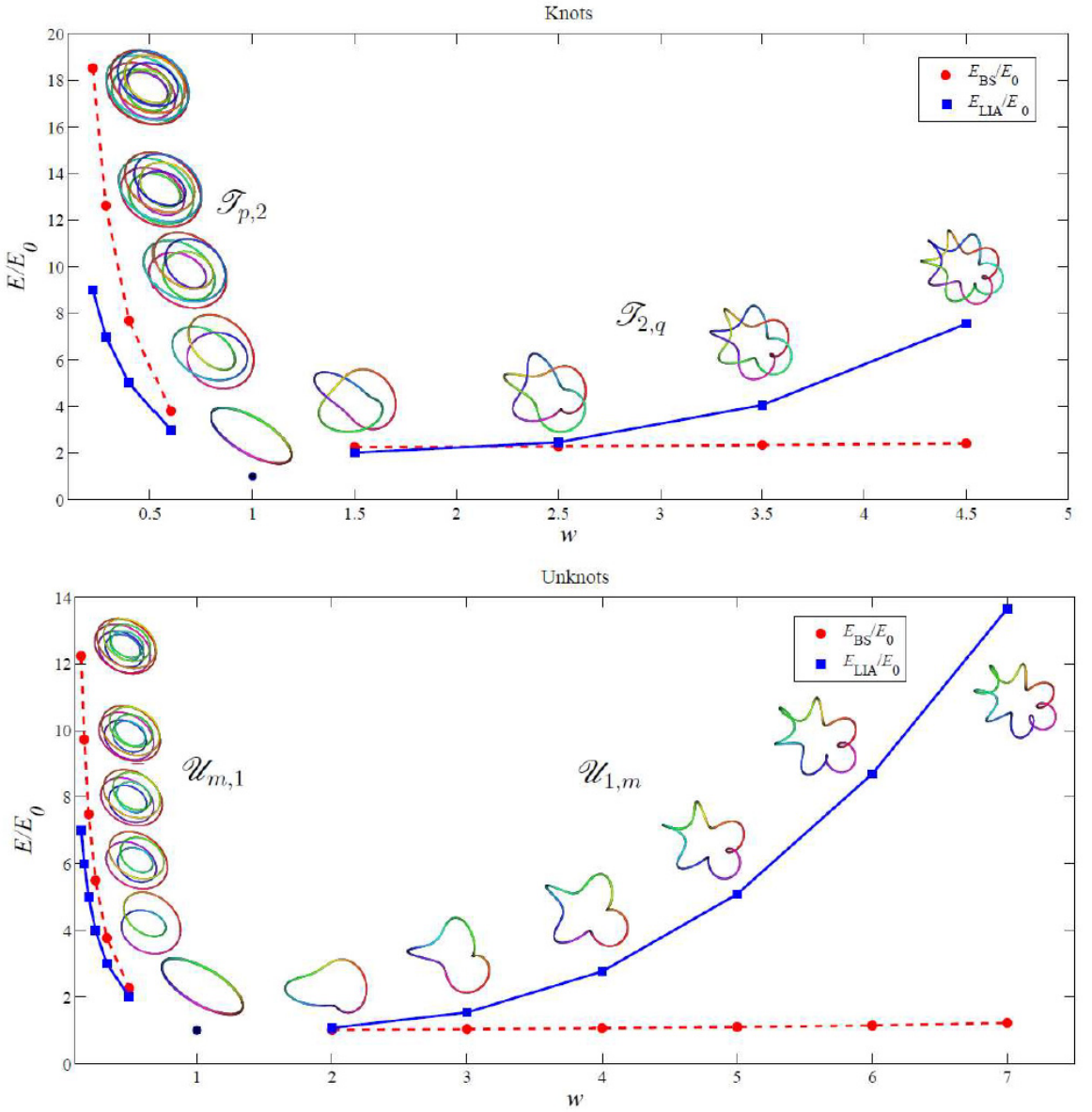

Fig. 7. Kinetic energy E of torus knots and unknots calculated by using respectively the Biot-Savart law and the LIA law (normalized with respect to the energy E_0 of the reference vortex ring), plotted against the winding number w ($p = 3, 5, 7, 9$; $q = 3, 5, 7, 9$; $m = 2, 3, \ldots, 7$). Interpolation lines are for visualization purposes only.

differences are essentially due to the contributions from the induction effects of nearby strands, captured by the BS law, but completely neglected under LIA.

4.4. Travelled distance before reconnection

Finally, we explore permanence of knot signature and occurrence of a reconnection event of vortex knots and unknots under both the BS and LIA law. Here we are interested to test not only conservation of topology, but also geometric signature and vortex coherence. Let us consider results shown in Figure 8. Since our results concern

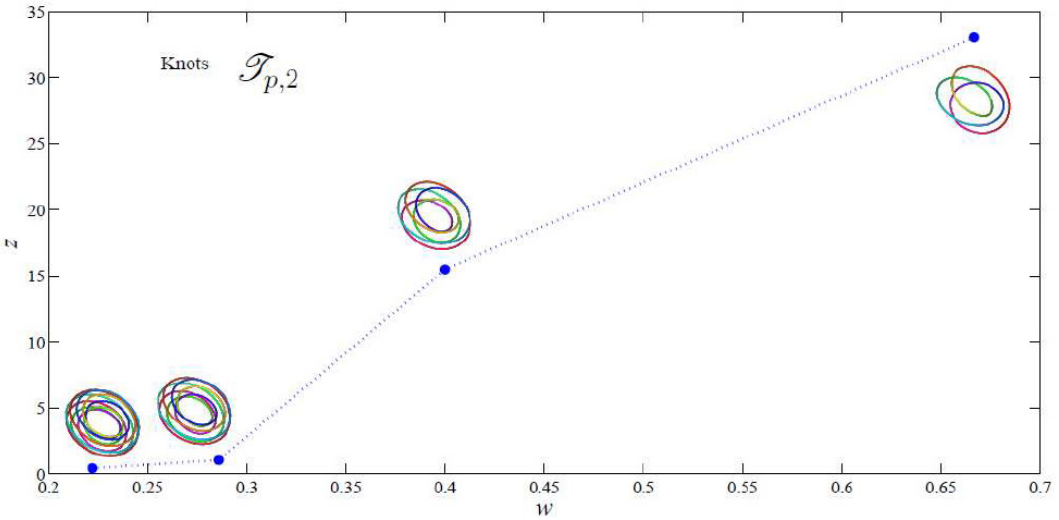

Fig. 8. Plots of the distance (z) travelled and time (t) elapsed before a reconnection event takes place for torus knots $\mathcal{T}_{p,2}$ ($p = 3, 5, 7, 9$), plotted against the winding number w. Calculations are based on the Biot-Savart law. Interpolation lines are for visualization purposes only.

both Euler's and superfluid dynamics, we remark that superfluid vortices *can* reconnect with each other in absence of dissipation [29, 30], whereas in the Euler context vortex topology is conserved; this important difference has been reviewed by Barenghi [31].

Here we adopt the following criterion: when, during the evolution, a vortex reconnection takes place, then we stop the calculation. Figure 8 shows the distance z travelled by the vortex during the computational time t till the first reconnection. We look for torus knots/unknots, that before a reconnection travel a distance z much larger than the typical vortex size.

We see that for $w < 1$ the space travelled tends to decrease with increasing knot complexity; for example $\mathcal{T}_{3,2}$ travels for 33 cm instead of 0.4 cm of $\mathcal{T}_{9,2}$. The computation has been extended to all the knots and unknots considered. All knots tested, including thosethat are LIA-unstable, are found to travel coherently for a long distance under the Biot-Savart law.

5. Conclusions

We have examined the influence of several geometric and topological aspects on the dynamics of vortex torus knots and unknots. This study is carried out by numerical integration of the Biot-Savart law, and by comparing the results for several knots and unknots with different winding numbers w. Generic behaviors are found for the class of knots/unknots tested.

Our numerical experiments clearly show that for $w < 1$ higher structural complexity induces faster motion, with torus knots and toroidal coils moving faster than the corresponding vortex ring $\mathcal{U}_0$. For $w > 1$ all vortex structures move essentially as fast as $\mathcal{U}_0$, almost independently from their total twist, that provides only a second-order effect on the dynamics. Since twist encapsulates torsion, this is consistent with the analysis and the results obtained by Ricca [32].

We have also found that for $w < 1$ vortex structures carry more kinetic energy than $\mathcal{U}_0$, whereas for $w > 1$ knots and poloidal coils have almost the same energy as $\mathcal{U}_0$. The LIA law under-estimates the energy of knots with $w < 1$ and over-estimates the energy for $w > 1$. The kinetic energy per unit length E/L has been found to be not constant.

Finally, we confirm that under the Biot-Savart law for all knots tested, including those LIA-unstable, are found to travel for several diameters before eventually unfolding and reconnecting.

Acknowledgements

FM would like to thank for the kind hospitality the Isaac Newton Institute for Mathematical Sciences, Cambridge (UK), where this work was carried out during the program "Topological Dynamics in the Physical and Biological Sciences" (16 July - 21 December, 2012). FM has been supported by a Cariplo Foundation (FYRE - "Fostering Young Researchers") project grant.

References

[1] Thomson W. Vibrations of a columnar vortex. *Phil. Mag.* 1980;10:155-168.
[2] Kaplanski F, Sazhin SS, Fukumoto Y, Begg SM, Heikal MR. A generalised vortex ring model. *J. Fluid Mech.* 2009;662:233-258.
[3] Hattori Y, Fukumoto Y. Short-wavelength stability analysis of a helical vortex tube. *Phys. Fluids*. 2009;21:014104-014110.
[4] Fukumoto Y, Moffatt HK. Kinematic variational principle for motion of vortex rings. *Physica D*. 2008;237:2210-2217.
[5] Walmsley PM, Golov AI, Hall HE, Levchenko AA, Vinen WF. Dissipation of quantum turbulence in the zero temperature limit. *Phys. Rev. Lett.* 2007;99(26):265302-265305.
[6] Barenghi CF, Sergeev YA. Motion of vortex ring with tracer particles in superfluid helium. *Phys. Rev. B.* 2009;80(2):024514-024518.
[7] Golov AI, Walmsley PM. Homogeneous turbulence in superfluid 4He in the low-temperature limit: experimental progress. *J. Low Temp. Phys*. 2009;156(3/4):51-70.
[8] Bewley GP, Sreenivasan KR. The decay of a quantized vortex ring and the influence of tracer particles. *J. Low Temp. Phys.* 2009;156:84-94.
[9] Tsubota M, Kobayashi M. Quantum turbulence in trapped atomic Bose-Einstein condensates. *J. Low Temp. Phys.* 2008;150:402-409.
[10] Mason PM, Berloff NG. Dynamics of quantum vortices in a toroidal trap. *Phys. Rev. A.* 2009;79:043620-043635.
[11] Horng T-L, Hsueh C-H, Gou S-C. Transition to a quantum turbulence in a Bose-Einstein condensate through the bending-wave instability of a single-vortex ring. *Phys. Rev. A.* 2008;77(6):063625-063628.
[12] Walmsley PM, Golov AI. Quantum and quasi-classical types of superfluid turbulence. *Phys. Rev. Lett.* 2008;100(24):245301-245308.
[13] Kida S. Stability of a steady vortex filament. *J. Phys. Soc. Jpn.* 1982;51:1655-1662.
[14] Calini A, Ivey T. Stability of small-amplitude torus knot solutions of the localized induction approximation. *J. Phys. A: Math Theor.* 2011;44(33):335204.
[15] Calini A, Keith SF, Lafortune S. Squared eigenfunctions and linear stability properties of closed vortex filaments. *Nonlinearity*. 2011;24:3555-3584.
[16] Barenghi CF, Vinen WF, Donnelly RJ. Friction on quantized vortices in HeII. *J. Low Temp. Physics*. 1982;52:189-247.
[17] Proment D, Onorato M, Barenghi CF. Vortex knots in a Bose-Einstein condensate. *Phys. Rev. E*. 2012;85:036306.
[18] Da Rios LS. Sul moto d'un liquido indefinito con un filetto vorticoso di forma qualunque. *Rend. Circ. Mat. Palermo* 1905;22:117-135.
[19] Fuller FB. The writhing number of a space curve. Proc. Nat. Acad. Sci. U.S.A. 1971;68(4):815-819.
[20] Ricca RL, Moffatt HK. The helicity of a knotted vortex filament. In: Moffatt HK, Zaslavsky GM, Comte P, Tabor M, editors. *Topological Aspects of the Dynamics of Fluid and Plasmas*. NATO ASI Series E: Applied Sciences vol. 218. Kluwer; 1992. p. 225-236.
[21] Kida S. A vortex filament moving without change of form. *J. Fluid Mech.* 1981;112:397-409.
[22] Ricca RL. Torus knots and polynomial invariants for a class of soliton equations. *Chaos*. 1993;3:83-91. [Also Erratum, *Chaos*. 1995;5:346.]
[23] Ricca RL. Geometric and topological aspects of vortex filament dynamics under LIA. in Meneguzzi M *et al.* editors. *Small-Scale Structures in Three-Dimensional Hydro and Magnetohydrodynamics Turbulence*, Lecture Notes in Physics vol. 462. Springer-Verlag, Berlin; 1995. p.99-104.
[24] Ricca RL, Samuels DC, Barenghi CF. Evolution of vortex knots. *J. Fluid Mech.* 1999;391:29-44.
[25] Schwarz KW. Three-dimensional vortex dynamics in superfluid helium. *Phys. Rev. B.* 1988;38:2398-2417.
[26] Maggioni F, Alamri SZ, Barenghi CF, Ricca RL. Kinetic energy of vortex knots and unknots. *Nuovo Cimento C* 2009;32(1):133-142.
[27] Maggioni F, Alamri SZ, Barenghi CF, Ricca RL. Velocity, energy, and helicity of vortex knots and unknots. *Phys. Rev. E*. 2010;82:026309.
[28] Barenghi CF, Ricca RL, Samuels DC. How tangled is a tangle? *Physica D*. 2001;157:197-206.
[29] Koplik J, Levine H. Vortex reconnection in superfluid helium. *Phys. Rev. Lett.* 1993;71:1375-1378.
[30] Bewley GP, Paoletti MS, Sreenivasan KR, Lathrop DP. Characterization of reconnecting vortices in superfluid helium. *Proc. Nat. Acad. Sci.* 2008;105:13707-13710.
[31] Barenghi CF, Is the Reynolds number infinite in superfluid turbulence? *Physica D*. 2008;237:2195-2202.
[32] Ricca RL. The effect of torsion on the motion of a helical vortex filament. *J. Fluid Mech.* 1994;273:241-259.